Interaction of Sedimentary Sulfides with Sea Water

By

Mustafa O. Moammar*

Abstract

Synthetic and natural ferrosphalerite particles, used in kinetic oxidation and hydrolysis studies in sea water, developed dense, crystalline coatings consisting of ordered and ferrimagnetic ૪ - (Fe, Zn) OOH. Due to the formation of this reactive diffusion barrier, the release of Zn^{2+} into solution decreases rapidly, and sulfide oxidation is reduced to a low rate determined by the diffusion of oxygen through the oxyhydroxide film. This also acts as an efficient solvent for ions such as Zn^{2+}, Ca^{2+} (and possibly Cd^{2+}), which contribute to the stabilization of the ૪ - (FeOOH) structure.

1. Introduction

The Red Sea contains extensive ore deposits that have motivated preparations for mining the seafloor; however, the unique geologic and oceanographic conditions that created these deposits have engendered a delicate ecosystem. In 1974 the Saudi-Sudanese Red Sea Commission was established for the dual purpose of efficiently recovering these resources while providing adequate protection of the marine environment. It was in the service of this latter objective that the present study was undertaken.

One of the most crucial questions in the disposal of marine tailings is the ultimate fate of the tailings and whether their heavy-metal contents remain stable in the solid phase or are leached out and enter the seawater column as dissolved ions.

Dissolved heavy metals are continuously put into the sea due to land erosion and hydrothermal and volcanic activity. Ocean sediments are well recognized as a major sink for formerly dissolved metals. The deep ocean's dissolved heavy metals are in extremely low concentrations and are expected to be in equilibrium with the seawater-sediment interface (Horne, 1969), which is controlled by the pH and Eh conditions in the overlying and interstitial seawater.

At mining the metalliferous mud must be diluted with seawater and brine in order to be pumped up from the seafloor, and must then be concentrated using the ultraflotation technique. The resulting tailings form a highly saline slurry with a density 5-10% higher than normal seawater and a solids content of 18-25 g/1, consisting mainly of aluminosilicates and other oxyanion compounds, with Ca^{2+}, Mg^{2+}, Fe^{2+} and Mn^{4+} as major cations (Table 1). Sulfides present due to incomplete separation were also observed

* Present address: Faculty of Marine Science, King Abdulaziz University, P.O.Box 1540, Jeddah - 21413, Saudi Arabia.

by X-ray diffraction of the tailing material, along with silicates, goethite, hematite, manganates, and some as yet unidentified phases (Fig. 1).

Table (1): Chemical Composition of Tailing Material*

Component	Range (%)	Average (%)
Compounds		
SiO_2	15.6 - 27.1	22.1
Ai_2O_3	1.2 - 4.1	2.6
CaO	3.2 - 8.6	5.8
MgO	1.0 - 2.1	1.5
Elements		
S	0.9 - 1.2	1.1
Fe	25.3 - 30.5	28.2
Mn	0.5 - 6.3	4.2
Zn	0.8 - 1.6	1.0
Cu	0.2 - 0.5	0.35
	(ppm)	(ppm)
Ag	20 - 50	35
Pb	40 - 70	60
Ni	5 - 70	25
Co	40 - 150	60
Cd	10 - 60	40

* Form Lange et al. (1980).

In an aerated and slightly alkaline environment (such as normal seawater), metal oxide and hydroxides are more stable than the metal sulfides, which are expected to undergo oxidation and dissolution until equilibrium is achieved. Based on this concept, an experiment was carried out to determine the rate at which sulfides in tailings are oxidized after discharge into seawater. The rate at which metal ions are released into solution at this reaction can be considered, as a measure of the environmental impact of sulfide discharge.
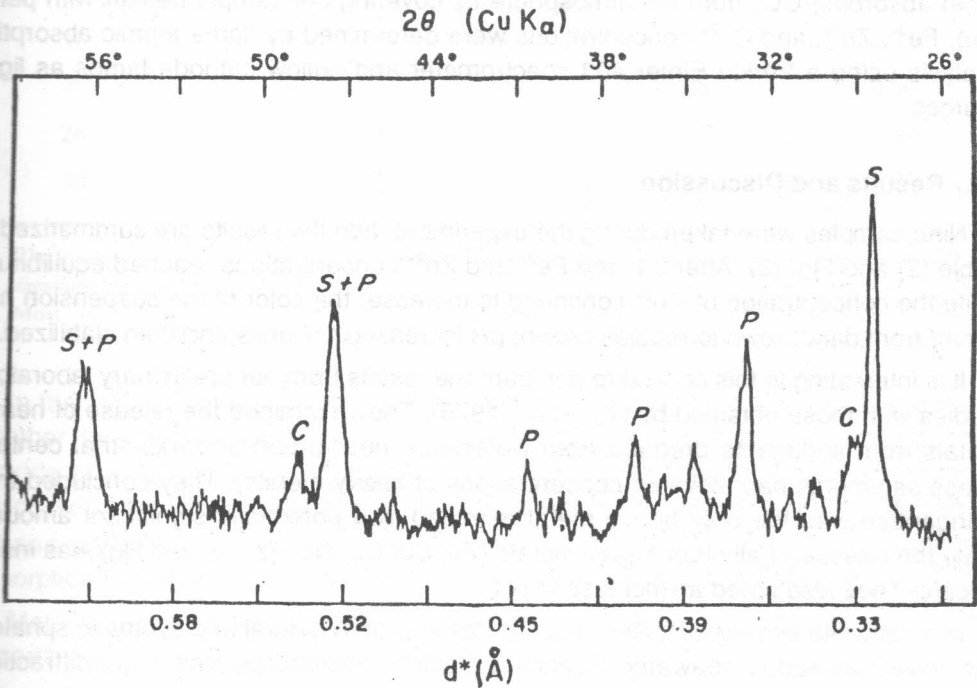
Figure (1)

X-ray diffractogram of sulfide concentrate obtained by removal of silicates from the tailing material of Mine Site IIIA. S=sphalerite; P=pyrite; C=chalcopyrite.

2. Oxidation Kinetics of the Tailing Material

2.1 - Experimental Procedures

One hundred millitiers of the original tailing suspension material* from Mine Site IIIA (in Atlantis II Deep) were diluted to one liter with distilled water and then placed in a water bath at a constant temperature of 45°C. This elevation of the experimental temperature to about 23°C above the temperature of the Red Sea deep water was arranged to accelerate the rate of oxidation by about a factor of four. The diluted tailing suspension was stirred and saturated with bubbling oxygen while evaporation was compensated for by adjusting the volume with additional distilled water. Twenty-five milliliters aliquots of the suspension were extracted at measured intervals.

The samples were filtered through 0.45-um millipore filters, and when the filtrate had cooled to ambient temperature (~ 22°C), pH was measured (care was taken to avoid absorbing CO_2 from the atmosphere by covering the sample beaker with parafilm). Fe^{3+}, Zn^{2+}, and Cu^{2+} concentrations were determined by flame atomic absorption analysis using a Perkin Elmer 403 spectrometer and hollow cathode lamps as light sources.

2.2 - Results and Discussion

Nine samples were taken during the experiment, and the results are summarized in Table (2) and Fig. (2). After 3 h, the Fe^{2+} and Zn^{2+} concentrations reached equilibrium, while the concentration of Cu^{2+} continued to increase; the color of the suspension had turned from dark brown to reddish brown; pH increased 1.7 units and then stabilized.

It is interesting in this context to compare the results from our preliminary laboratory studies with those obtained by Lee et al. (1975). They examined the release of heavy metals from sediments dredged from waterways near urban and industrial centers (these sediments had elevated concentrations of heavy metals). They concluded that manganese was the only heavy metal released in a potentially significant amount, while the release of all other heavy metals (Zn, Cd, Cu, Ni, Pb, Fe, and Hg) was insignificant. They also noted an increase in pH.

In a separate experiment, Red Sea sulfides and both natural and synthetic sphalerites were oxidized in seawater. Scanning electron microscope and x-ray diffraction analysis of the oxidized material revealed that elemental sulfur formed together with zinc hydroxide when ZnS was used as the solid phase to be oxidized, and with γ- (Fe, Zn) OOH when (Zn, Fe) S was used as reactant solid. When the γ- (Fe, Zn) OOH layer forming on the sphalerite crystals in the oxidizing solution becomes sufficiently thick, diffusion of the dissolved reaction products through this barrier is impeded, and further release of zinc ions essentially ceases. These experiments will be discussed in greater detail in the next section.

---

* The tailing charcteristics were described by J. Lange et al., 1980; see also Table (1) and Fig. (1).

Table (2): Kinetics of the Release of H^+, Cu^{2+}, and Zn^{2+} into Solution upon Oxidation and γ - FeOOH Barrier Formation on Tailing Sulfide Particles

Time (hr)	pH	Concentration (u M/1)		
		Fe**	Zn	Cu
1/6	5.8	34.02	1.53	0.28
1/2	6.2	32.23	1.99	0.31
2	7.0	30.44	2.29	0.38
3	7.5	28.65	3.06	0.44
6	7.5	29.54	3.52	0.52
8	7.4	28.65	3.06	0.60
24	7.5	27.75	3.06	1.89
30	7.4	28.65	3.52	1.73

* The temperature of the suspension was 45°C, and oxygen saturation was maintained by oxygen bubbling. The measured composition was that of the filtrate.

** Most of the iron in the filtrate was probably present in colloidal than ionic solution.

In the complex phase mixture that the tailings comprise, it is difficult to determine whether the iron and zinc ions are being precipitated in solid solution in a single oxyhydroxide phase, which was found to be the case in the single-crystal experiments (discussed further in section 3.4), or as separate phases. The presence of clay minerals and manganates in the tailings also makes it necessary to consider the possibility of sorption by these minerals of ions released from the sulfides at oxidation.

Metal ions precipitating as hydroxides in aqueous solution usually produce H^+ ions, according to the following general reaction:

$$M^{n+} + n\,H_2O = M\,(OH)^{\circ}n + nH^+$$
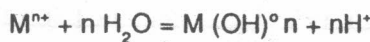
Additional protons may be released by sorption of metal ions in exchange with the bound OH groups on the hydrous oxide surface as follows:

$$\equiv Me - OH + M^{n+} = \equiv Me - OM^{(n-1)+} + H^+.$$
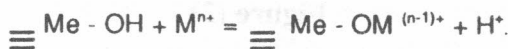
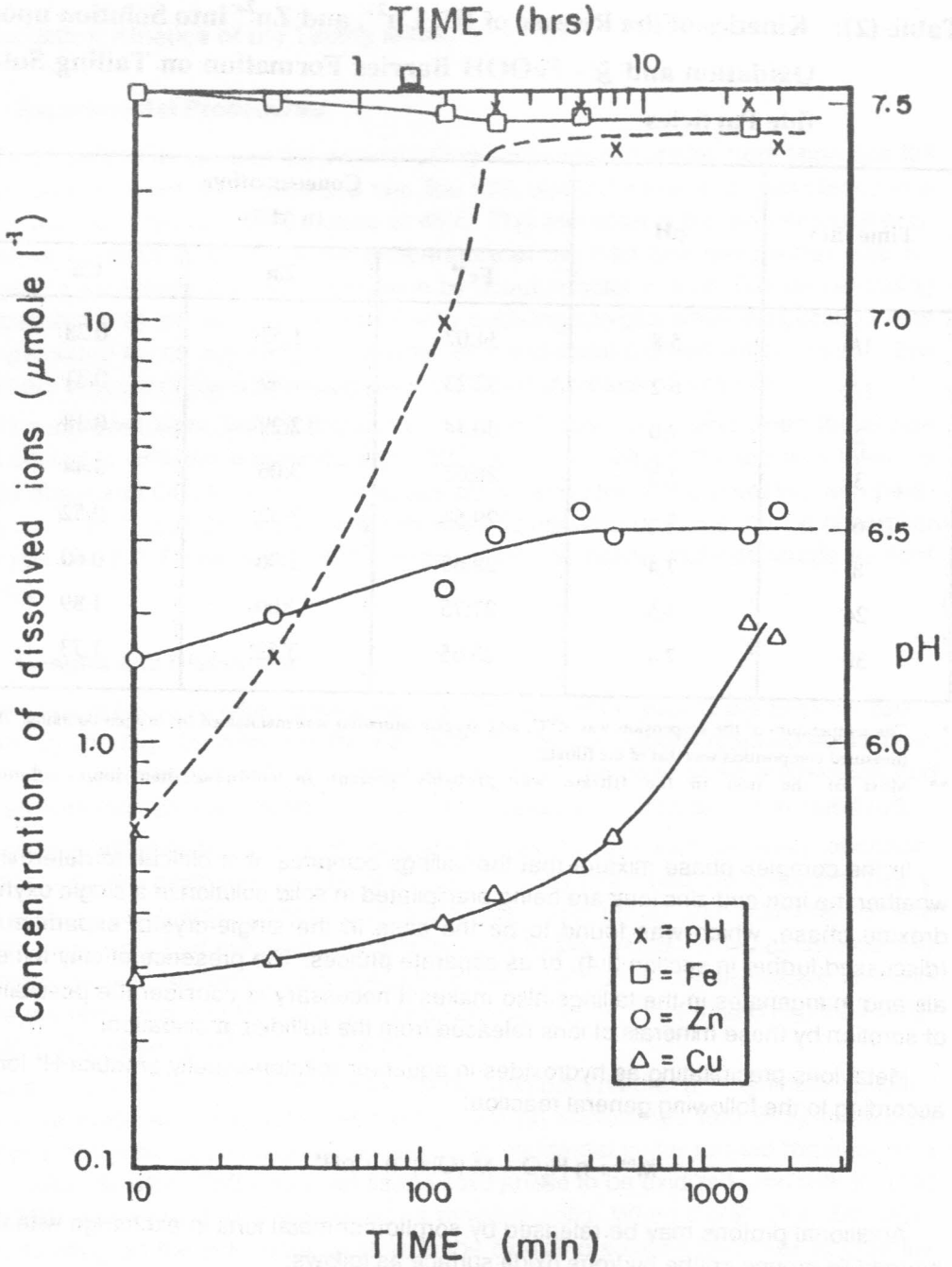in which M is the metal ion sorbed and $\equiv$ Me - OH the metal oxyhydroxide site.

Figure (2)

Time-dependent release of ions at oxidation of sulfudes in sediment-brine suspension diluted with deionized water. T=45 °C.

According to Hodgson et al. (1964), the reactions between metal ions and clay mineral surfaces are likely to be one of two types:

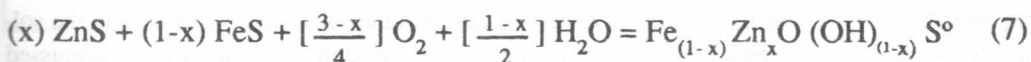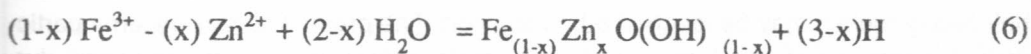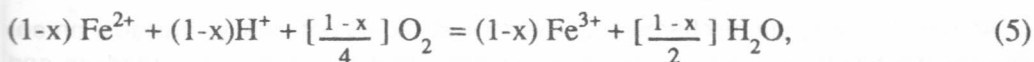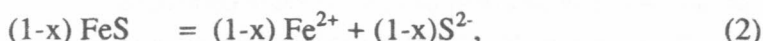(1) adsorption of a hydrolyzed ion, which may be written as

$$M^{2+}H_2O = MOH^+ + H^{+}{}^+$$
$$MOH^+ + X^- = XMOH$$
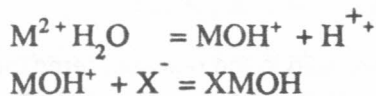
(Where X^- represents a negatively charged adsorbing surface);

(2) specific exchange of an unhydrolyzed ion with weakly dissociable H+, which may be written as:

$$M^{2-} + HX = M^-X + H^+ .$$

In all of the above-discussed processes associated with the removal of metal ions from solution, protons are released, leading to a decrease in pH. Concurrent processes, which do not entail release of protons, are due to the oxidation of metal and sulfide ions:

$$(x) ZnS = (x) Zn^{2+} + (x) S^{2-} \tag{1}$$

$$(1-x) FeS = (1-x) Fe^{2+} + (1-x)S^{2-}, \tag{2}$$

$$(x) S^{2-} + (1-x) S^{2-} + 2H^+ = H_2S, \tag{3}$$

$$H_2S + 1/2 O_2 = S^\circ + H_2O, \tag{4}$$

$$(1-x) Fe^{2+} + (1-x)H^+ + [\tfrac{1-x}{4}] O_2 = (1-x) Fe^{3+} + [\tfrac{1-x}{2}] H_2O, \tag{5}$$

$$(1-x) Fe^{3+} - (x) Zn^{2+} + (2-x) H_2O = Fe_{(1-x)}Zn_x O(OH)_{(1-x)} + (3-x)H \tag{6}$$

$$(x) ZnS + (1-x) FeS + [\tfrac{3-x}{4}] O_2 + [\tfrac{1-x}{2}] H_2O = Fe_{(1-x)}Zn_x O (OH)_{(1-x)} S^\circ \tag{7}$$

The important role of these proton-consuming reactions during the oxidation and hydrolysis of the tailing material is shown by the stability in pH when synthetic (Zn, Fe) S is oxidized in distilled water or seawater and by the observations of elemental sulfur (aS) produced in the reaction.

3. Oxidation of Sphalerite (Zn, Fe) S in Seawater

3.3 - Environmental Aspects and General Considerations

Oxidation of insoluble transition metal sulfides, particularly in a closed system, leads to the release of protons. The increased acidity may be caused by simple hydrolysis of the metal ion or by precipitation of an insoluble oxide or hydroxide. The extent of acidity depends on the nature of the metal ion, especially on the degree of its hydrolysis or on the insolubility of its oxide or hydroxide. At complete oxidation the for-

mation of sulfate ion contributes to the acidity. Thus, reaction (4) in Section 2, in the presence of excess oxygen, takes the course.

$$H_2S + 2O_2 = SO_4^{4-} + 2H^+. \tag{8}$$

With the presence of the free acid in the reaction, ferric ion will, instead of FeOOH, produce hematite, a - Fe_2O_3, which remains highly insoluble even at a low pH. Zinc, which does not readily substitute in hematite will then prevail as Zn^{2+} or $ZnOH^+$, causing a high zinc concentration in solution if the system remains closed.

In an open seawater-oxygen system with metal sulfides in the proportions given above, the seawater possesses a substantial buffering capacity and its pH is not markedly altered by the acidity yielded by reaction (8). In addition, reaction (4) is more likely to take place in seawater, and under these conditions oxygen consumption is one-fouth of that in reaction (8).

The sulfur formed by reaction (4) is taken out of seawater temporarily by organisms and assimilated into sulfur-bearing proteins; most of this organic sulfur is oxidized and returned to the sea when the organisms die (Loyed, 1967), but some may be fixed in organic sediments or by the conversion of inorganic sulfur into sulfide and its precipitation as metal sulfide under oxygen deficient conditions.

In our experiments, aiming at modeling the actual sulfide release conditions, the ratio seawater/sulfide was kept large. As a result of the buffering by seawater, and the formation of elemental sulfur (Fig. 4b), pH remained almost constant during the oxidation reaction which practically ceased when the sulfide particles at this pH became effectively passivated by the γ- FeOOH barrier layer.

As noted earlier, the discharged sulfide minerals could potentially constitute an environmental hazard since they are not in equilibrium with the aqueous medium and their heavy metals may be leached out in solution. The present study concerns particularly the behavior of sphalerite (which is the major sulfide phase in the solid ore) during oxidation in seawater, and the solubility of zinc and the solid phases that control the solubility. A set of experiments was arranged to study these questions, and they will be discussed in some detail below.

3.2 - Experimental Procedures

Precautions were taken to avoid contamination, especially in those procedures that affected the analysis of zinc solubility. Samples of synthetic sphalerite with different iron contents (prepared using the synthesis procedure discussed in Moammar 1985), natural sphalerite and natural marcasite, were oxidized in 4l of seawater that had been filtered through a 0.22- um membrane filter. Oxygen was provided by the addition of 2 M H_2O_2 or by saturation with bubbling oxygen, and the reaction took place at room temperature (22°C). The suspension was stirred during the experiments.

Natural marcasite (FeS_2), producing FeOOH upon oxidation, was mixed with natural sphalerite in those experiments which aimed at assessing the effect of excess iron oxyhydroxide on zinc solubility in seawater.

174

Table (3) summarizes the different experimental conditions. Two 1-liter samples were taken from each experiment for zinc and iron analysis by atomic absorption spectroscopy, the first sample after 5 weeks and the second after 10 weeks. The samples were filtered through 0.22-um membrane filters, and the dissolved iron and zinc were concentrated by a factor of 200 using ammonium salt of the dithiocarbonate of pyrrolidine (APDC) for coprecipitation (Boyle and Edmond, 1977).

Table (3): Summary of Experimental Conditions in Sulfide Oxidation

Experiment	Reaction solid*	Sphalerite (Zn, Fe)S		Buffer solid	Fe/Zn in solid	Reactant oxidant
		Compositon (M)	Sample weight			
1	S. sphalerite	100% ZnS	100 mg	–	0	2% H_2O_2
2	S. sphalerite	80% ZnS, 20% FeS	100 mg	–	0.21	2% H_2O_2
3	S. sphalerite	75% ZnS, 25% FeS	100 mg	–	0.28	Oxygen
4	N. sphalerite	76% ZnS, 24% FeS[1]	1 g	–	0.27	2% H_2O_2
5	N. sphalerite and marcasite	76% ZnS, 24% FeS[1]	100 mg	FeS_{2i} 50 mg	0.72	Oxygen
6	N. sphalerite and marcasite	76% ZnS, 24% FeS[1]	100 mg	FeS_{2i} 500 mg	2.92	Oxygen

* S, sypthetic; N, natural. Note: The grain size was less than 10 um for all experiments with the exception of experiment 4 (grain size less than 1 mm).
1 Estimated from ao measurements using the correlation ao = 5.4091 + 0.00046 X, where X is the M of FeS (Moammar, 1981).

At the end of each experiment, the oxidation products were washed several times with distilled water and stored dry at room temperature for subsequent analysis of their crystal structure and compositon.

3.3 - Results and Discussion

In general, within three days the suspension of ≤ 10-um dark gray (Zn, Fe) S changed to dark brown; millimeter-sized black sphalerite grains, which were also used in the experiment, became covered with a reddish-brown coating within a week.

3.3.1 - Analysis of Zinc Concentration In Solution

Atomic absorption spectroscopy was carried out with a Perkin Elmer instrument using a hollow cathode lamp for the light source. Table (4) summarizes the results. The fact that the results after 5 weeks are identical to those after 10 weeks indicates that the reaction had practically ceased in 5 weeks or less.

In Experiment 1. in which pure synthetic ZnS was oxidized, the zinc concentration in solution was 2.4 uM, which is the $Zn(OH)_2$ saturation level in seawater. In preliminary experiments we verified the solubility data in the literature by the addition of $ZnCl_2$ (50 uM) to seawater at pH 8 to make a metastable solution. These experiments showed that, after the addition of zinc ion, the zinc hydroxide forms rapidly, with a concurrent drop in the zinc concentration to the equilibrium value of about 3 uM/liter.

Table (4): Release of Zinc into Seawater during Sulfide Oxidation[1]

Experiment	Fe / Zn in sulfide charge	[Zn] (nM)	
		5 weeks	10 weeks
1	0	3×10^3	2.9×10^3
2	0.21	35.9	36.7
3	0.28	34.7	34.4
5	0.72	26.0	27.5
6	2.92	16.4	15.3

(1) At 25°C and a pH of 8.2

For the cases in which (Zn, Fe) S was the solid sulfide, the zinc concentration decreased exponentially with the increase of iron in the system, reaching a lowest value of ~ 15 nM/liter (see Table 4 and Fig. 3). During oxidation and release of iron and zinc from the sulfide material, it appears (from the solubility and

crystal structure) that the zinc is incorporated in solid solution in the crystalline FeOOh that forms as a reaction product. The polymorph formed in Experiments 2 and 3 (where Fe/Zn < 0.3 in the sulfide charge) is found to be γ (Fe, Zn) OOH (see Fig. 4). The γ - FeOOH phase can accommodate up to 40 mole % Zn^{2+} for Fe^{3+} in the structure, forming delta - (Fe, Zn) OOH (Muller et al., 1979).

The highest zinc concentration in the solution (36 nM) was found in equilibrium with the most highly Zn-substituted compound $[Fe_{0.7} Zn_{0.30} (OH)_{0.7}]$. Similarly, experiment 2,
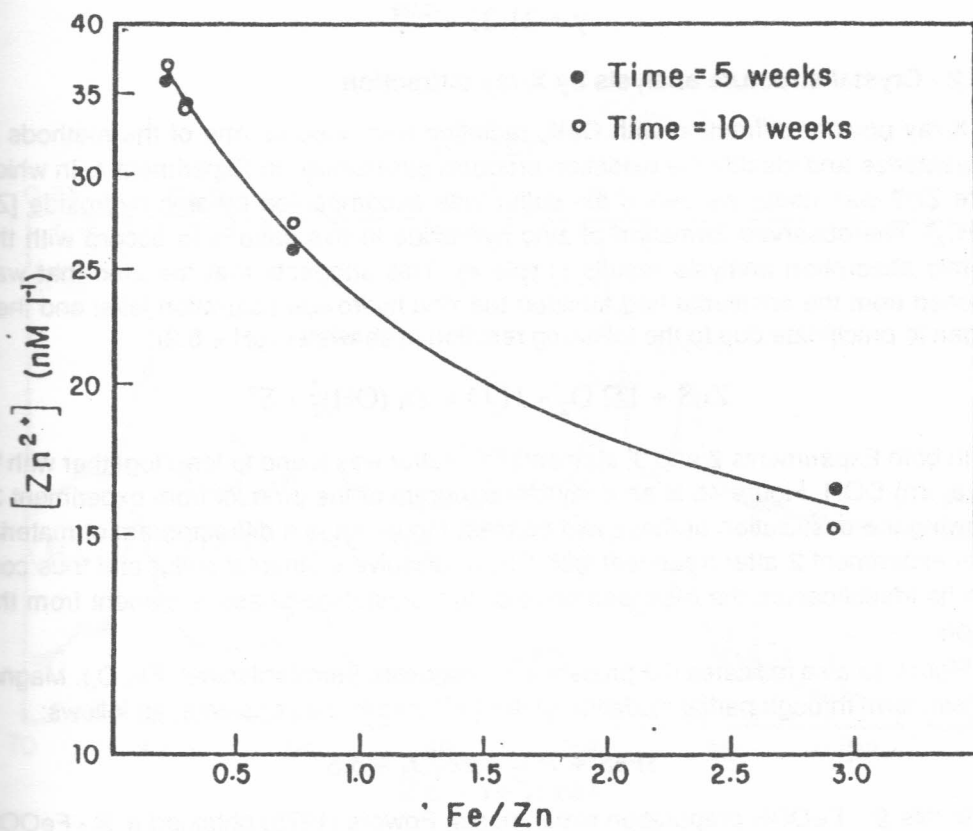
Figure (3)

Effect of the iron content of solid ractants on the solubility of zinc at oxidation of iron-zinc sulfide in seawater. The temperature was 22 °C, the pH was 8.2; measurements were made after 5 and 10 weeks.

representing the solubility of δ - (Fe, Zn) OOH formed from oxidation of $(Zn_{0.8} Fe_{0.2})$ S in seawater, gave the same high extreme value of 36 nM. With decreasing zinc substitution in the oxyhydroxide, the solubility of Zn gradually decreased through Experiments 5 and 6 (Fig. 3), reaching the lowest value measured (15.3 nM) at the lowest zinc concentration in the sulfide source material with Fe/Zn = 2.92. This ratio was achieved by using a mixed charge of FeS and $(Fe_2 Zn_{0.8})$ S as a solid reactant.

Consequently, as expected, the concentration (y) of zinc in solution in equilibrium with (Fe, Zn) OOH is a function of the zinc concentration (x) in this solid. The relationship, empirically established from these experiments, is

$$y = 21.35\ e^{-0.13r}$$

3.3.2 - Crystal structure analysis by X-ray diffraction

X-ray powder diffraction with CuK_a radiation was used as one of the methods to characterize and identify the oxidation products structurally. In Experiment 1, in which pure ZnS was used, elemental a - sulfur was accompanied by zinc hydroxide [Zn $(OH)_2$]. The observed formation of zinc hydroxide in this case is in accord with the atomic absorption analysis results (Table 4). This suggests that the zinc that was leached from the sphalerite had attained the zinc hydroxide saturation level and then began to precipitate due to the following reaction in seawater (pH = 8.2):

$$ZnS + 1/2\ O_2 + H_2O = Zn\ (OH)_2 + S°.$$

In both Experiments 2 and 3, elemental a - sulfur was found to form together with δ - (Fe, Zn) OOH. Figure 4b is an x-ray diffractogram of the product from experiment 3, showing the association of these two phases. Figure 4a is a diffractogram of material from experiment 2 after treatment with CS_2 to dissolve elemental sulfur and thus confirm its identification; the disappearance of this crystalline phase is evident from the graph.

Figure 4a also indicates the presence of magnetite (ferroferrispinel, $Fe_3 O_4$). Magnetite can form through partial oxidation of the Fe^{2+} ions in the sphalerite, as follows:

$$3FeS + 2O_2 = Fe_3O_4 + 3\ S°$$
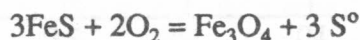
In this δ - FeOOH preparation experiments, Powers (1975) obtained a δ - FeOOH together with magnetite. Also, Feitknecht (1959) obtained δ - FeOOH (together with magnetite) from Fe $(OH)_2$ in amounts inversely proportional to the rate of oxidation. The δ - FeOOH present in experiments 2 and 3 (Fig. 4) was formed by oxidation of sphalerite. These results stimulated further investigation of the δ - FeOOH structure and its solid solution when Zn^{2+} was substituted for Fe^{3+} (see Moammar 1985).

3.3.3 - Single-crystal analysis of structure and composition

The X-ray powder diffraction analysis integrates over a large number of crystallites; it does not give direct information on the chemical composition of individual crystals
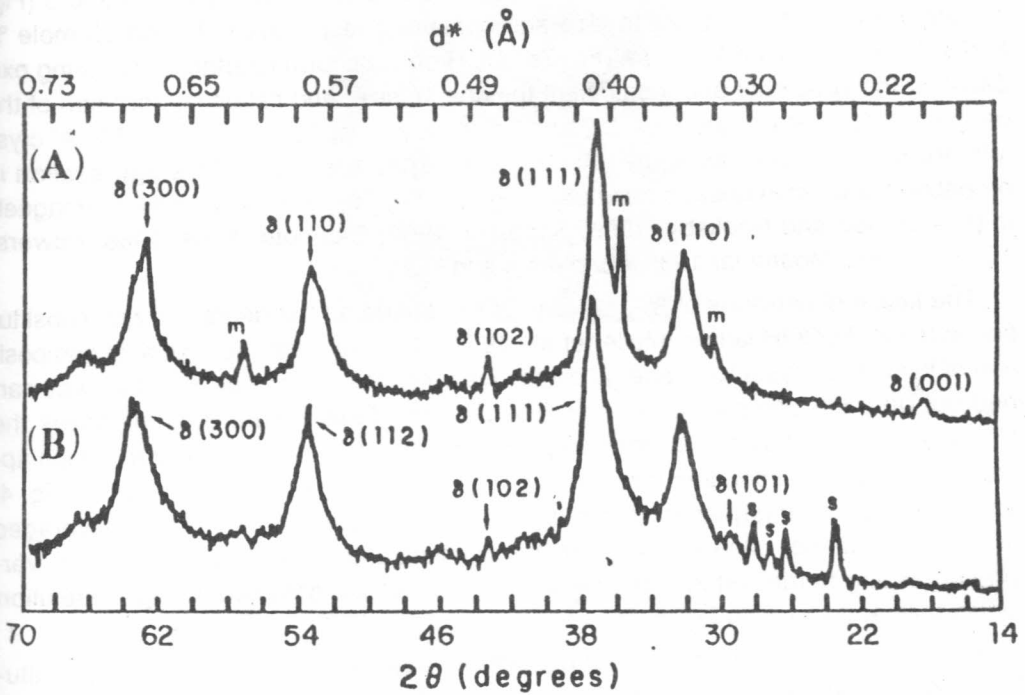
Figure (4)

X-ray diffractogram of the phases resulting from oxidation of synthetic (Zn,Fe)S in seawater with 2% H_2O_2.:

(a) Reaction products from Experiment 2 where the reactant sulfide (sphalerite) had the composition $(Zn_{0.80}, Fe_{0.20})S$. Elemental sulfur was removed from this sample by CS_2 treatment.

(b) From Experiment 3 with composition $(Zn_{0.75}, Fe_{0.25})S$. ϒ = ϒ'-(Fe,Zn)OOH; S-rhombic sulfur; m = magnetite.

and is incapable of detecting crystallites smaller than a fraction of 1 um when CuK_a radiation is used. The study of the γ- (Fe, Zn) OOH was therefore supplemented with transmission electron microscopy (TEM), selected-area electron diffraction (SAED), and energy-dispersive x-ray fluorescence spectrometry (EDAX). Using these high-resolution techniques it was possible to analyze single crystals of the phases in question. A Hitachi-H 500 transmission electron microscope operated at 100 kV and combined with an Ortec detector with multichannel analyzer was used in the analysis.

Dried samples from experiments 2 and 3 were crushed between glass slides and then ultrasonically dispersed in distilled water. Small samples of the homogeneous suspension were transferred by pipet into nylon or copper grids that were covered with formvar film. When dry, some of the specimen grids were coated with gold to serve as an internal standard.

The synthetic sphalerite crystals used in Experiments 2 (Figs. 5 and 6) and 3 (Fig. 7) ranged from 0.1 to 0.5 um in size and contained respectively 20 and 25 mole % FeS substituting for ZnS. The γ- (Fe, Zn) OOH crystals form topotactically during oxidation of the sphalerite and thus inherit the shape, size, and cation composition of the parent sulfide crystals (see Figs. 2.7 and 2.8 in Moammar 1985). The 500-700 A° crystals are seen to occur as aggregates in both Fig. 5 and Fig. 6. This aggregation is probably due to spontaneous magnetization; γ - (Fe, Zn) OOH is strongly ferrimagnetic (Francombe and Rooksby, 1959; Simpson, 1962; Okamoto, 1964, 1968; Powers, 1975; see also Moammar 1985, chapters 4 and 5).

The lattice dimensions of γ - (Fe, Zn) OOH depend on the degree of zinc substitution in the γ- FeOOH lattice (Muller et al., 1979). To determine the chemical composition of individual crystallites, energy dispersive x-ray absorption spectrometry was carried out on each particle that was analyzed by the TEM. Figure 8, summarizes the EDAX results as ratios of the emission power of ZnK relative to Fe radiation, which approximate the corresponding mass fraction ratios. In the x-ray diffraction data (Fig. 4, and Table 5), the interplanar spacings represent the unit cell dimensions averaged over a large number of crystallites, with composition, and therfore cell parameters, varying according to the distribution of individual crystallites, obtained by high resolution techniques and shown in Fig. 8.

Muller et al. (1979) established a correlation between the degree of zinc substitution and the unit cell parameters of synthetic γ - FeOOH. Unit cell volume has been chosen here instead of the a_o and c_o parameters as an appropriate measure of the zinc content of the structure. As shown in Fig. 9, the correlation between cell volume and composition derived here is in excellent agreement with that calculated from the data of Muller et al. (1979).

The zinc content in the γ - (Fe, Zn) OOH phase in Experiment 2 (Figs. 5 and 6) is much higher than that in Experiment 3 (Fig. 7), presumably because of corresponding differences in the zinc content of the two ferrosphalerite sources. This is also reflected in the structure, in that the (001) line in the x-ray diffraction pattern of the γ - (Fe, Zn) OOH phase is clearly present in Fig. 4 (Experiment 2). Muller et al . (1979) reported
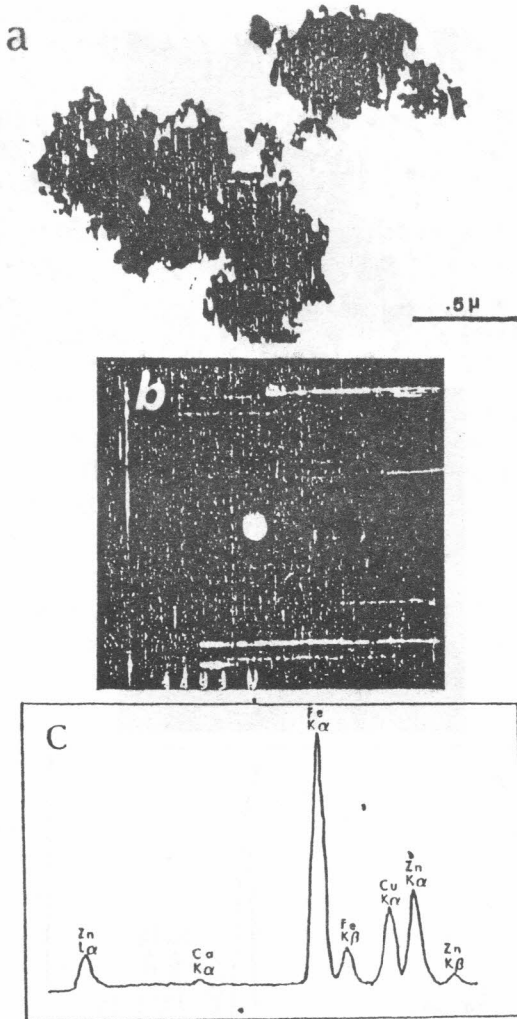
Figure (5)

(a) Transmission electron micrograph of γ-(Fe,Zn)OOh formed during oxidation of $(Zn_{0.80}.Fe_{0.20})S$ in seawater,, as indicated in Table 3 (Experiment 2); the spots (100-200 °A in size) that appear in the micrograph are from gold crystals.

(b) Electron diffraction pattern of the central region of the micrograph. The subscripts d and g to the Miller indices refer to γ-(Fe,Zn)OOH; and gold.

(c) Energy-dispersive spectrometer tace of γ-(Fe,Zn)OOH. The Cu K emission is due to the copper grid support.

Figure (6)

(a) Transmission electron micrograph of γ-(Fe,Zn)OOh formed during oxidation of $(Zn_{0.80}.Fe_{0.20})S$ in seawater,, as indicated in Table 3 (Experiment 2); the spots (100-200 °A in size) that appear in the micrograph are from gold crystals.

(b) Electron diffraction pattern of the central region of the micrograph. The subscripts d and g to the Miller indices refer to γ-(Fe,Zn)OOH; and gold.

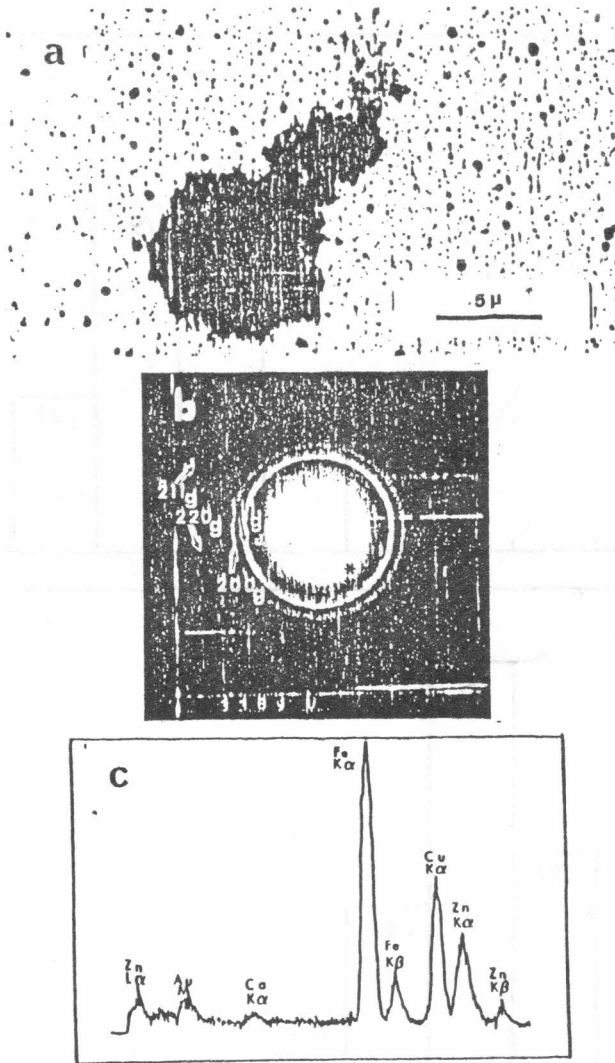(c) Energy-dispersive spectrometer tace of γ-(Fe,Zn)OOH. The Cu K emission is due to the copper grid

Figure (7)

(a) Transmission electron micrograph of γ-(Fe,Zn)OOh formed during oxidation of $(Zn_{0.75},Fe_{0.20})S$ in seawater, as described in TAble 3; the spots (100-200 °A in size) that apear in the micrograph are gold crystals.

(b) Electron diffraction pattern of the upper right edge of the crystal aggregate, showing the prism reflections (h00, hk0, 0k0) of γ-(fe,Zn)OOH and the diffraction rings from poly-crystalline gold, used as diffraction standard (subscripts g).

(c) Energy-dispersive spectrometer trace of γ-(Fe,Zn)OOH. The Cu K emission is from the sample grid. In addition to Zn. Ca (from the seawater) also substitutes in these crystals.
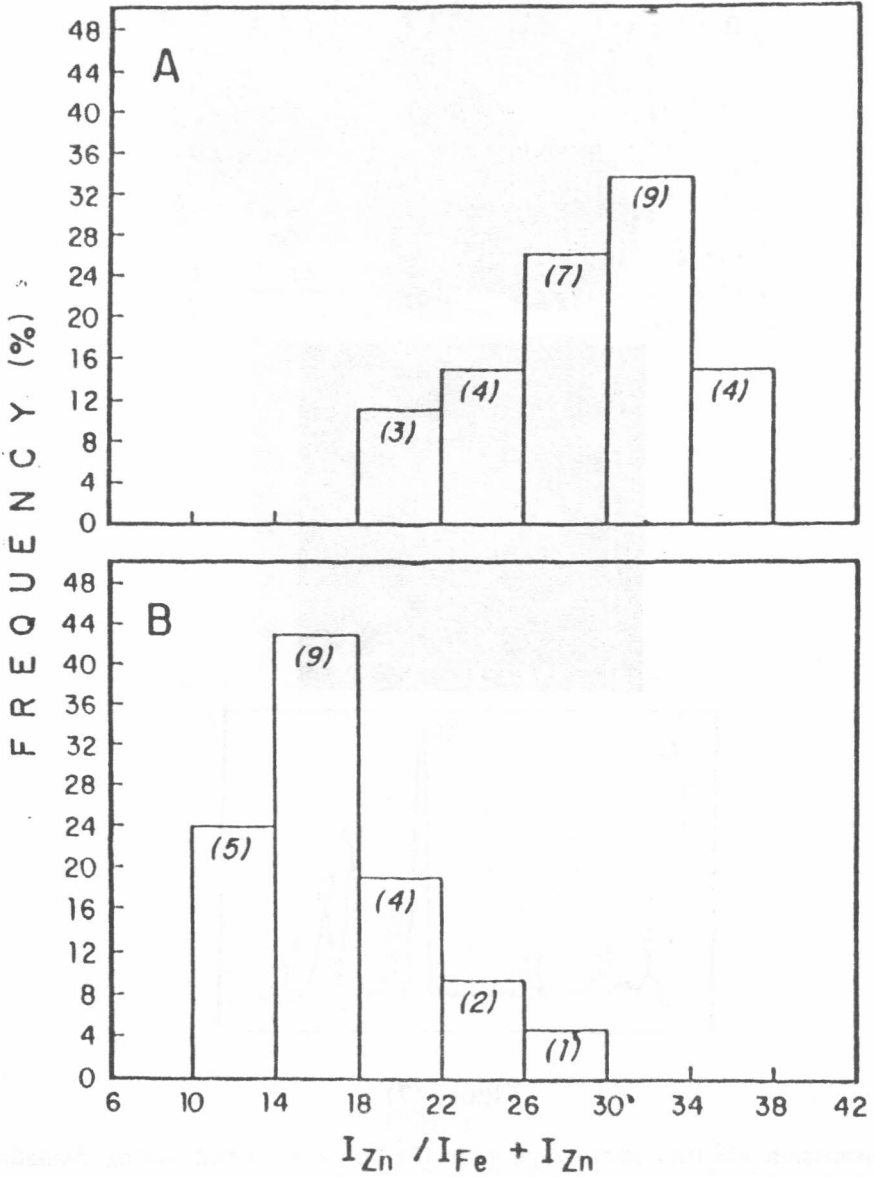
Figure (8)

Frequency distribution of Zn /(Fe+Zn) K_a intensity ratios in individual ɤ -FeZnOOH crystals measured by x-ray fluorescence in STEM. The numbers in parentheses refer to the number of crystal analyzed in Experiment 3.
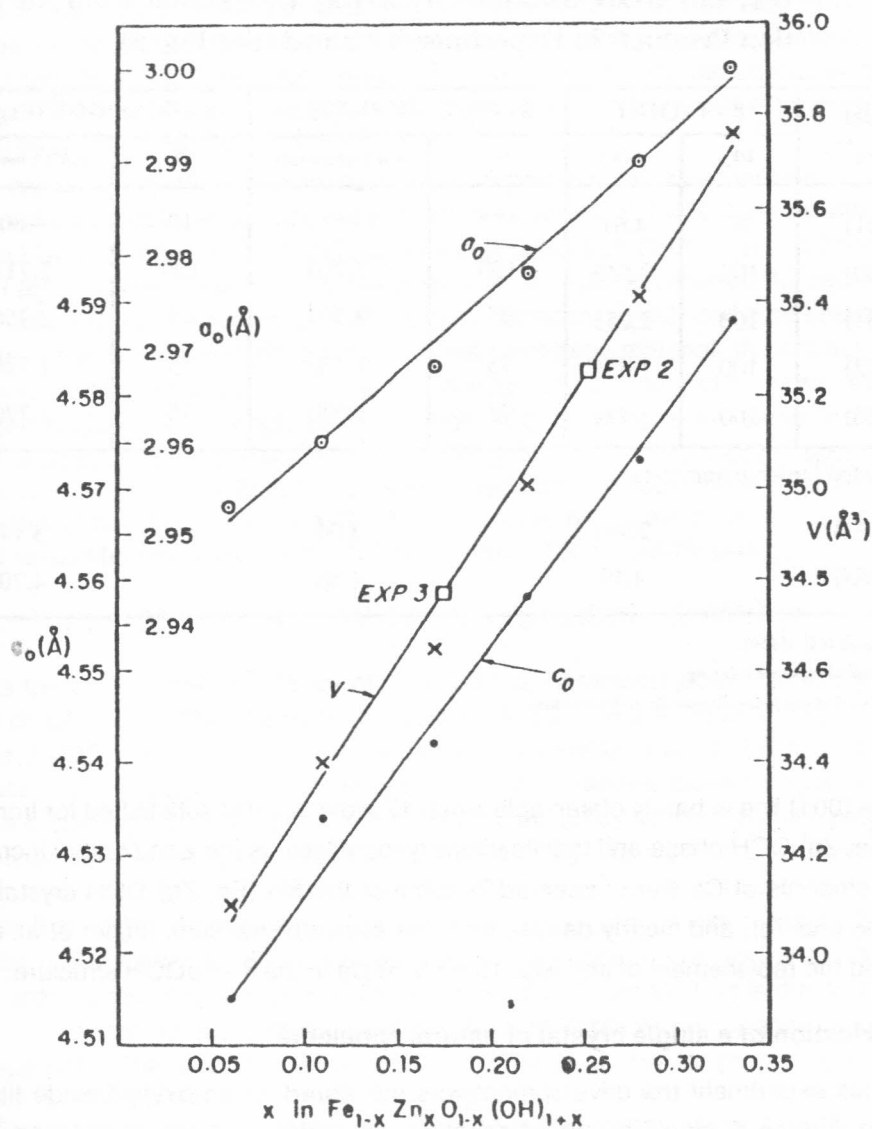
Figure (9)

Correlation between the degree of zinc substitution and the unit cell parameters of synthetic γ - FeOOH (V=unit cell volume). Data from Experiments 2 and 3 and from Muller et al., 1979.

Table (5): Structral Data 8 - FeOOH* and the Derivative Structure of 8 - (Fe, Zn) OOH Obtained by X-Ray Diffraction from the Reaction Products in Experiments 2 and 3 (See Fig. 3)

Miller index**	8 - FeOOH		8 - (Fe, Zn)OOH (Exp.3)		8 -(Fe, Zn)OOH (Exp.2)	
	1/1.	d (A')	1/1.	d(A') (observed)	1/1.	d(A') (observed)
(001)	20	4.61	***	***	10	4.80
(100)	100	2.545	100	2.710	100	2.711
(101)	100	2.255	75	2.300	75	2.350
(102)	100	1.685	75	1.729	75	1.720
(110)	100	1.471	75	1.520	75	1.770
Calculated lattice parameters						
ao (A•)		2.941		3.04		3.14
co (A•)		4.49		4.56		4.70

* From Bernal et al. (1959).

** Fundamental structure indexing.

*** Not observed due to insufficient Zn in the structure.

that the (001) line is barely observable when 17 mole % Zn is substituted for iron in the 8 - (Fe, Zn) OOH phase and that its intensity increases as the zinc content increases. Minor amounts of Ca were observed in some of the 8 - (Fe, Zn) OOH crystals (see Figs. 6c and 7c), and clearly derives from the seawater medium. Muller et al. (1979) reported the replacement of iron with 10 mole % Ca in the 8 - FeOOH structure.

3.4. Oxidation of a single crystal of natural sphalerite

In this experiment the development was monitored on an oxyhydroxide film of a uniform surface of single crystal of sphalerite at oxidation. A large, polished crystal (about 1 cm in diameter) of the same natural sphalerites used in Experiments 4-6 (see Table 3) was placed in filtered seawater and saturated with bubbling oxygen. After 3 days a rust film of FeOOH coated the crystal surface, but it was still thin enough to be translucent. After a week, the film was opaque. The film was then gently rinsed with deionized water and stripped from the crystal with plastic replicating tape, which was subsequently placed on a carbon film resting on the copper grid used for electron microscopy.

The micron-size crystals of synthetic sphalerite used in Experiments 2 and 3 (see Figs 2.3 and 2.6) reacted to form g-(Fe,Zn) OOH crystallites as small as 500-700 A° (Figs. 3.5, 3.6, and 3.7) upon oxidation in seawater. In contrast, surface oxidation of the large single crystal of natural sphalerite resulted in the formation of much larger (0.5 to 1 um) euhedral platelike crystals of 8 - (Fe,Zn) OOH with hexagonal symmetry (see Figs. 10a and 11a). The symmetry and orientation of the crystals was revealed by electron diffraction (see Figs 10b and 11b).

The crystal in Fig. 11 was exposed to vapor-deposited gold as an internal standard. The observed interplanar spacings are given in column 2 of Table 6 along with those observed by Chukhrov et al. (1977) by electron diffraction from synthetic Zn-free 8 - FeOOH (column 4 in Table 6). Two major differences appear between the two sets of data in the table. First, only two sets of the prism reflections (hk0) could be obtained by Chukhrov et al. by electron diffraction from their synthetic material. In contrast seven reflections in this C-axis zone were strong enough to be recorded by sharp electron diffraction spots from the single crystal in Figs. 10b. attesting to the exceptioally high degree of order attained at the present mode of growth of 8-(Fe,Zn)OOH. Second, the $a.$ parameter of the 8-(Fe,Zn)OOH is as expected from the substitution (Fig. 11c). larger than that of the unsubstituted 8-FeOOH measured by Chukhrov et al. This size difference is manifested in all of the (hk0) reflections, which together give

$$a. [8- (Fe.Zn)OOH] \quad 5.25A°\pm0.02 \quad 8 \quad a.(8\text{-}FeOOH) \quad 5.08A°\pm0.01$$

Note the enlargement b a factor of $\sqrt{3}$ of the a_o parameter from 2.94 in the fundamental structure to 5.08 in the superstructure for 8-FeOOH and from 3.03 to 5.25 for 8-(Fe,Zn)OOH. Because of this enlargement, Chukhrov et al. (1977) proposed the existence of two delta-iron oxyhydroxides, both with hexagonal close packing and both of same $c.$ parameter: ordered 8-FeOOH, characterized by its ferrimagnetic properties and enlargement of the a_o-parameter from 2.94 to A° by a factor $\sqrt{3}$ (column 4 in Table 6), and less ordered, nonmagnetic 8'-FeOOh, where the $a.$ parameter is 2.94°A (column 8 in Table 6). However, bernal et al (1959) and others (Francombe and Rooksby, 1959; Okamoto, 1964; Muller et al., 1979) chose 2.94A° as the $a.$ parameter for the ordered ferrimagnetic 8-FeOOH (column 10 in Table 6). This is due to the fact that in their diffraction patterns (col. 7-8 and 9-10 in Table 6) no superstructure lines were apparent. The evidence on which Chuckhrov et al. rely for proposing a superstructure is the observation of a diffraction ring at 3.1A°, ascribed to (101) in their polycrystalline sample (column 4 in Table 6). Due to our success in slow crystallization of well-ordered 8(Fe,Zn)OOH, seven prism reflections (hOO) and (hkO) were observed in this work, including the fundamental superlattice (100) (Figs. 10b and 11b; column 2 in Table 6). These data clarify the relationship between the superstructure and the fundamental structure (columns 5 and 6, respectively, in Table 6), and gives further support to the interpretation by Chukhrov et al, by adding two more lines (200) and (210) that are unique to the supercell. The pyramid reflection (101) observed by Chuckhrov et al. could obviously not be observed in our specimens, since they are well ordered single crystals, oriented with the C-axis parallel to the electron beam.

Table (6): Electron and X-ray Diffraction Characteristics of Ordered Ferrimagnetic δ- FeOOH and δ-(Fe, Zn) OOH Compared to the Less. Ordered Nonferrimagnetic δ-FeOOH

Superstructure					Fundamental Structure				
Col.1	2	3	4	5	6	7	8	9	10
δ-(Fe,Zn)OOH[a]		δ-FeOOH[b]		Miller index	Miller index	δ-FeOOH[e]		δ-FeOOH[d]	
I	d(A°)	I	d(A°)	(hkl)	(hkl)	I	d(A°)	I	d(A°)
e		10	4.5	(001)	(001)			20	4.61
S	4.56			(100)					
e		20	3.1	(101)					
VS	2.61	100	2.54	(110)	(100)	100	2.54	100	2.545
e		50	2.22	(111)	(101)	50	2.23	100	2.255
W	2.28			(200)					
e		40	1.68	(112)	(102)	30	1.70	100	1.685
W	1.72			(210)					
MS	1.51	90	1.47	(300)	(110)	90	1.47	100	1.471
W	1.31			(220)	(200)			20	1.271
W	1.26			(310)	(310)			20	1.271
5.25 A°		5.08 A°		ao parameter		2.93A°		2.941A°	

(a) Formed at ferrosphalerite - seawater oxidation and hydrolysis (see Figs. 10b and 11b).

(b) Synthetic 8-FeOOH formed by rapid oxidation of Fe (OH)2 in a strongly alkaline medium (Chukhrov et al., 1977).

(c) Natural 8-FeOOH from the Pacific Ocean (Chukhrov et al., 1977).

(d) Synthetic 8-FeOOH formed by rapid oxidation of Fe (OH)2 in a strongly alkaline medium (Bernal et al., 1959).

(e) Not visible due to the orientation of the crystal with the basal plane (001) normal to the electron beam (see Figs. 10b and 11b).

Note: All data were obtained by electron diffraction with the exception of those of Bernal et al., which were obtained by x-ray diffraction.

The structurally related natural mineral described by Chukhrov et al. (1977) as δ'-FeOOH, or ferroxyhyte, appears to be a paramagnetic solid without notable cation or vacancy ordering, in contrast to the well-ordered, strongly ferrimagnetic phase prepared in the present work, which was also found as a mineral for the first time in the oxidized sediment from the black smokers on the deep sea foor (see Sect. 4 below).

The superstructure most likely results from the way cations are ordered relative to the vacancies in the δ-(Fe,Zn)OOH. Such ordering of the Zn-Fe pairs is probably also
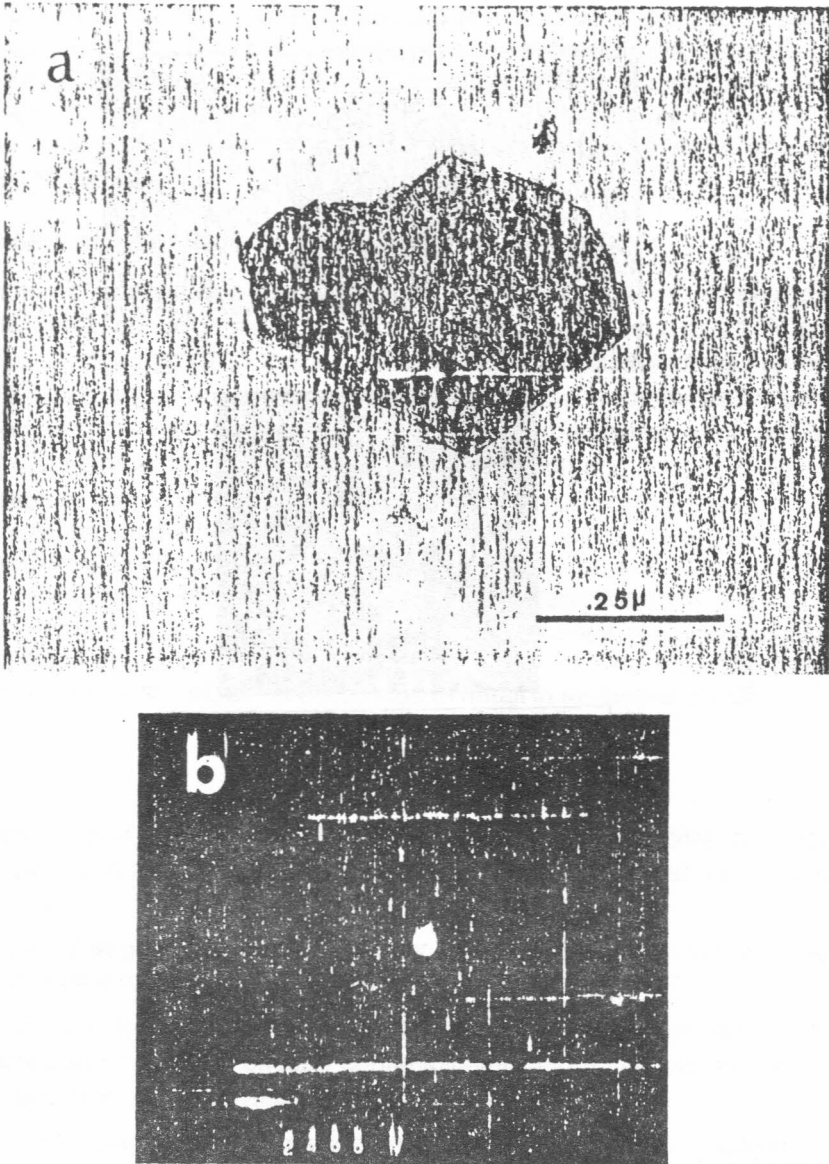
Figure (10)

(a) Transmission electron micrograph of a euhedral of crystal of ᵹ-(FeZn)OOH formed during oxidation of natural sphalerite in seawater, as described in Section 3.4.

(b) Electron, diffraction pattern outlining the reciprocal lattice of the ᵹ-(Fe-,Zn)OOH single crystal (shown in a). The innermost sharp hexagonal spots are attributable to the (100). reflection and are not seen in the less well-ordered ᵹ-FeOOH crystals reported by Chucrov et al. (Column 4 in Table 6).
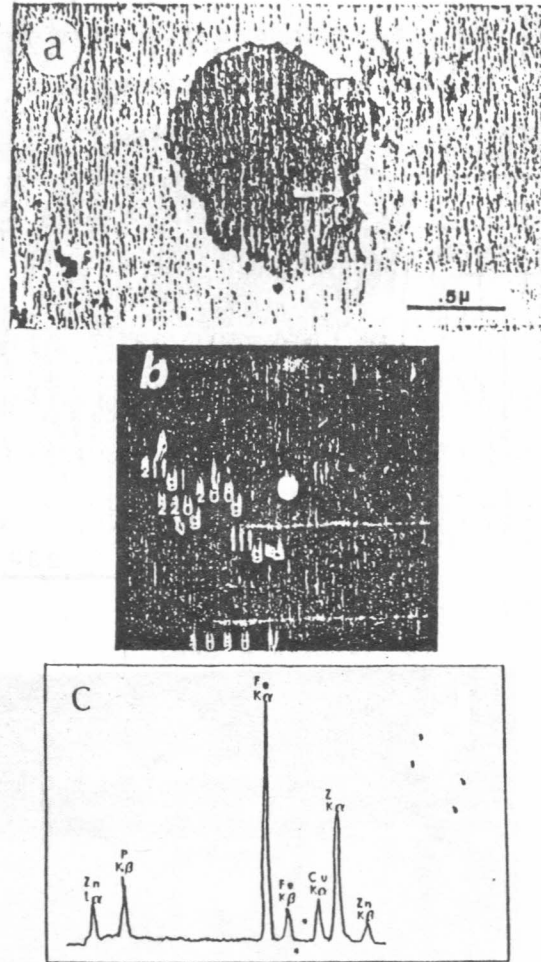
Figure (11)

(a) Transmission electron micrograph of a euhedral of γ -(FeZn)OOH formed during oxidation of natural sphalerite in seawater.

(b) Electron, diffraction pattern of the micrograph showing two rationally offeset single-crystal domains with parameters as listed in Table 6. The indexed circles labeled g are composite reflections from the goldfilm crystallites deposited onto the sample for diffraction calibration.

(c) Energy dispersive spectrometer trace of γ -(Fe, Zn) OOH. The K emission from phosphorus is due to the plastic replicating tape used to strip off the γ -(Fe, Zn) OOH film; and the Cu emission derives from the support grid.

responsible for the strong ferrimagnetism in δ-(Fe,Zn)OOH (Okamoto, 1964, 1968:see also Moammar 1985). Similarly, vacancy ordering in the Zn-free synthetic δ-FeOOH prepared by Chukhrov et al. (1977) and Bernal et al. (1959) is probably responsible for the strong ferrimagnetism in the pure δ-FeOOH and a superstructure is also expected here. Bernal et (1959) could not observe the superstructure, possibly due to the poor quality of the crystals.

4. Formation of -(Fe,Zn)OOH as a mineral on the sea floor

Oxidation of sulfide minerals under conditions similar to those studied experimentally in this work, occurs in many seafloor spreading areas, such as 21 °N on the East Pacific Ridge. In these areas the old surfaces of the sulfide chimneys are found to be covered by an orange stain, and sediment near the base of the nonactive vents is also found to consist of what has been referred to as "amorphous iron oxide and hydroxide" (RISE Project Group 1980; Findel et al., 1980; Haymon and Kaster, 1979 and 1981). Examination of this iron oxyhydroxide shows that it contains substantial amounts of δ -(Fe,Zn)OOH, often coating particle cores of unaltered sulfide. This finding, for the first time, establishes δ-(Fe,Zn)OOH as a well ordered mineral, arising from slow oxidation of sulfide minerals on the seafloor in accord with prediction from laboratory experiments (Moammar, 1981). It also confirms the significance of the diagenesis experiments reported above as models for the natural process. The separation and characterization of natural δ-FeOOH is descussed in detail in Moammar (1985).

References

Arrhenius, G. and Tsai, A. (1981). Structure, phase transformation and prebiotic catalysis in marine manganate minerals. Rep. Scripps Inst. Oceanography 81-82.

Bernal, J.D., Dasgupta, D.R. and Mackay, A.L. (1959). The oxides and hydroxides of iron and their structural inter-relationships. Clay Minerals Bull. 4, 15-30.

Boyle, E.A. and Edmond, J.M. (1977). Determination of copper, nickel and cadminum in seawater by APDC chelate coprecipitation and flameless atomic absorption spectrometry. Analytica Chimica Acta 91, 189-197.

Chukhrov, F.V. Zvvagin, B.B. Gorshkov, A.I., Yermilova, L.P., Karovushkin, V.V., Rudnitskaya, Ye. S., and Yakubovskaya. N. Yu. (1977). Feroxyhyte, a new modification of FeOOH. International Geology Review 19, 873-890.

Crane, S. (1981). "Structural Chemistry of the Marine Manganate Minerals". Ph. D. Thesis, Univ. of California, San Diego, California, 296 pp.

Feltknecht, W. (1959). Ueber die Oxidation von festen Hydroxydverbindungen des Eisens in wassrigen Losungen. Z. Electrochem 63d (1).

Francombe, M.H., and Rooksby, H.d. (1959). Structure transformation effected by the dehydration of diaspore, goethite, and delta ferric oxide. Clay Minerals. Bull. 4, 1-14.

Giovanoli, R., and Brutsh, R. (1979). L'echange des ions de transition par le manganate--10 ˚A et le manganate--7 ˚A. In "La Genese des Nodules de Manganese" (C. Lalou, ed., Collop, Internat. du CNRS, No. 289, Gif-sur-Yvette, September, 1979, 305 pp.

Hodgson, J.F., Tiller, K.G., and Fellows, M. (1964). The role of hydrolysis in the reaction of heavy metals with soil-forming materials. Soil Sci. Proc. 28, 42-46.

Lange, J., Baccker, H., Post, J., and Weber, H. (1980). Plans and tests for a metal concentration and tailing disposal at sea. Symp. Coastal Mar. Environ. Red Sea, Gulf of Aden and Trop. West. Ind. ocean. Khartoum.

Lee, G.F., Lopez, J.M., and Mariani, g.M. (1975). Leaching and bioassay studies on the significance of heavy metals in dredged sediments. Toronto, Proc. International Conference on Heavy Metals in the Environment, pp. 731-764.

Moammar, M/.O. (1981). "Environmental Aspects of mining in the Red Sea, Seawater-metal sulfide interaction". M.S. Thesis, Univ. of California, San Diego, California, 168 pp.

Moammar, M.O. (1985). "Marine Diagenesis of Hydrothermal Sulfide". Ph. D. Thesis, Univ. of California, san Diego, California, 219 pp.

Muller, O., Wilson, R., and Krakow, W. (1979). γ-FeO(OH) and its solid solutions. Part 1, Preparation and crystal chemistry. Journal of Materials Science 14, 2929-2936.

Okamoto, S. (1964). Studies on γ-iron oxyhydroxide (Third report), Journal of the chemical Sosiety of Japan, Industrial Chemistry Section 67 (11), 1855-1860.

Okamoto, s., (1968). Structure of γ-FeOOH. Journal of the American Ceramic Society 51. 594-599.

Powers. D.A. (1974). "Magnetic Behavior of Basic Iron (III) compounds". Ph. D. Thesis, Calif. Inst. Technol., Pasadena, California., 322 pp.

Simpson, A.W. (1962). Some superparamagnetic properties of fine particle γ-FeOOH. Journal of Applied Physics 33, 1203-1205.